Multispectral fluorescence sensitivity to acidic and polyphenolic changes in Chardonnay wines – The case study of malolactic fermentation

Maxime Pacheco, Pascale Winckler, Ambroise Marin, Jean-Marie Perrier-Cornet, Christian Coelho

MULTISPECTRAL FLUORESCENCE SENSITIVITY TO ACIDIC AND POLYPHENOLIC CHANGES IN CHARDONNAY WINES – THE CASE STUDY OF MALOLACTIC FERMENTATION

PACHECO Maxime[1], WINCKLER Pascale[1,2], MARIN Ambroise[1,2], PERRIER-CORNET Jean-Marie[1,2], COELHO Christian[1,3,*]

[1] *UMR Procédés Alimentaires et Microbiologiques, AgroSup Dijon, Université de Bourgogne Franche-Comté, 1 Esplanade Erasme, 21000 Dijon, France.*

[2] *Dimacell Imaging Facility, AgroSup Dijon, Université de Bourgogne Franche-Comté, 1 Esplanade Erasme, 21000 Dijon, France.*

[3] *Current address :* Université Clermont Auvergne, INRAE, Vetagro Sup campus agronomique de Lempdes, UMR F, F-15000 Aurillac, France.

* Corresponding author :

Christian Coelho, Université Clermont Auvergne, INRAE, Vetagro Sup campus agronomique de Lempdes, UMR F, F-15000 Aurillac, France, christian.coelho@vetagro-sup.fr

Abstract :

In this study, stationary and time-resolved fluorescence signatures, were statistically and chemometrically analyzed among three typologies of Chardonnay wines (A, B and C) with the objectives to evaluate their sensitivity to acidic and polyphenolic changes. For that purpose, a dataset was built using Excitation Emission Matrices of fluorescence (N=103) decomposed by a Parallel Factor Analysis (PARAFAC), and fluorescence decays (N=22), mathematically fitted, using the conventional exponential modeling and the phasor plot representation.

Wine PARAFAC component C4 coupled with its phasor plot g and s values enable the description of malolactic fermentation (MLF) occurrence in Chardonnay wines. Such proxies reflect wine concentration modifications in total acidity, malic/lactic and phenol acids. Lower g values among fresh MLF+ wines compared to MLF- wines are explained by a quenching effect on wine fluorophores by both organic and phenolic acids. The combination of multispectral fluorescence parameters opens a novel routinely implementable methodology to diagnose fermentative processes.

Keywords :

Malolactic fermentation - organic acids – traceability - PARAFAC components - fluorescence lifetime – phasor plot

1. Introduction

Fluorescence spectroscopy techniques offer the advantage of a fast, robust and non-destructive characterization ability over expensive and time-consuming separative techniques. Their high sensitivity and specificity are important and allow the study of fluorescent compounds and chemical families among the complex chemistry present in food matrices and particularly wine. Over the past decade, much has been written on fluorescence usefulness in providing helpful classification indicators regarding cultural practices, varieties distinction, technological practices, regional authentication, adulteration and spoilage problematics (Airado-Rodríguez, Durán-Merás, Galeano-Díaz, & Wold, 2011; Cabrera-Bañegil, Valdés-Sánchez, Moreno, Airado-Rodríguez, & Durán-Merás, 2019; Coelho, Aron, Roullier-Gall, Gonsior, Schmitt-Kopplin, & Gougeon, 2015; Elcoroaristizabal, Callejon, Amigo, Ocana-Gonzalez, Morales, & Ubeda, 2016; Mierczynska-Vasilev et al., 2021; Moret et al., 2019; Ranaweera, Gilmore, Capone, Bastian, & Jeffery, 2021; Robert-Peillard, Boudenne, & Coulomb, 2014; Saad, Bouveresse, Locquet, & Rutledge, 2016; Sadecka, Jakubikova, & Majek, 2018; Santos, Bosman, Aleixandre-Tudo, & du Toit, 2022; Wan, Pan, & Shen, 2012; Zhong et al., 2014).

From a practical point of view, fluorescence spectroscopy is classically used by winegrowers and winemakers to help them in their decision-making process. For instance, red grape maturity can be estimated using anthocyanins and chlorophyll steady state fluorescence proxies (Agati et al., 2013; Agati, Meyer, Matteini, & Cerovic, 2007). Trivellin *et al.* used the fluorescence lifetime variations of a metal/porphyrin complex to measure oxygen concentrations in wine fermentation and ageing tanks (Trivellin et al., 2018). This technology is widely used in wine industries for dissolved oxygen measurement during winemaking steps and wine bottling. The detection of wine yeasts and bacteria is also based on the steady state fluorescence response of labelled microorganisms, sorted by a flow cytometer and used by several oenological laboratories (Longin, Petitgonnet, Guilloux-Benatier, Rousseaux, & Alexandre, 2017). Other applications consist~~ed~~ in analysing the total steady state fluorescence of wines using Excitation Emission Matrices of fluorescence (EEMF) coupled to multivariate approaches in order to discriminate grape varieties, vintages, oenological or fermentation practices (Airado-Rodríguez, Galeano-Díaz, Durán-Merás, & Wold, 2009; Coelho et al., 2015). The measurement of fluorescence lifetimes of wine chemicals (resveratrol, flavylium and pyranoflavylium cations) when adsorbed on clay fining agents or adsorbents enabled the study of organic complexations and organic/inorganic interactions (Silva et al., 2019; Trigueiro et al., 2018). Some authors tried to relate wine fluorescence patterns to wine quality and to wine chemical composition (Coelho et al., 2015; Coelho, Gougeon, Perepelkine, Alexandre, Guzzo, & Weidmann, 2019; Elcoroaristizabal et al., 2016; Saad et al., 2016; Sadecka et al., 2018).

Among the qualitative criteria enhancing wine quality, malolactic fermentation (MLF) is often achieved in cellars by endogenous or exogenous lactic acid bacteria, reducing acidity by conversion of malic acid into lactic acid and increasing organoleptic properties by generating new volatile compounds (Bauer & Dicks, 2017). MLF is a fermentative process that brings a reorganisation of the chemical composition of wines and contributes to flavour complexity. During this fermentative process, the phenolic profile of wines evolves and depends on the strains of lactic bacteria realizing MLF (T. Hernández, Estrella, Pérez-Gordo, Alegría, Tenorio, & Moreno-Arribas, 2007). MLF has been shown to influence the concentrations of hydroxycinnamic acids and their derivatives, increasing the concentrations of caffeic/p-coumaric/ferulic acids and decreasing those in their precursors such as caftaric/coutaric/fertaric acids (Cabrita, Torres, Palma, Alves, Patão, & Costa Freitas, 2008; Teresa Hernández, Estrella, Carlavilla, Martín-Álvarez, & Moreno-Arribas, 2006; T. Hernández et al., 2007; Martínez-Pinilla, Martínez-Lapuente, Guadalupe, & Ayestarán, 2012). MLF can also be accompanied by a wood contact time in wines providing novel sensory attributes to Chardonnay wines (González-Centeno, Chira, & Teissedre, 2019). Additionally MLF could distinguish cool-climate and warm-climate wine producing regions in the world (Bartowsky, 2005). In those regions, differences in malic lactic consumption and derived metabolisms during berry maturation phase, would increase the chemical variability on grapes and therefore on MLF+/-Chardonnay wines on a world scale (Bartowsky, 2005; Ruffner, 1982). For that reason, the use of high-throughput fluorescence spectroscopic techniques to diagnose an elevated number of diverse wine samples combining chemometric tools, appears to be a good alternative to evaluate both MLF+/- wine discrimination and associated chemical modifications.

In this paper, we discuss the application of multispectral fluorescence with chemometrics to differentiate Chardonnay wines based on their acidic modification once malolactic fermentation was achieved (MLF+) or not (MLF-). For that purpose, Excitation Emission Matrices of fluorescence (N=103) were decomposed by a Parallel Factor Analysis (PARAFAC) and fluorescence lifetime decays (N=22) were mathematically fitted, using the conventional exponential modeling and the phasor plot representation. The chemical significance of MLF discrimination among Chardonnay wines by multispectral fluorescence was evidenced by organic acids and polyphenol concentration measurement on the analyzed wines.

2. Materials and Methods

2.1 Wine Samples

One hundred and three Chardonnay wines were analyzed in this study gathering three typologies of Chardonnay wines, named as A, B and C wines. Twelve fresh wines during vintage 2021 from two

Burgundian wineries, Jean Claude Boisset at Nuit Saint Georges (named as A) and Domaine de l'Université de Bourgogne at Marsannay La Côte (named as B), were sampled before (MLF-) and after (MLF+) malolactic fermentation. Ninety-one Chardonnay wines were sampled during the "Chardonnay du Monde 2018" wine contest (named as C) organized in March 2018 at Chateau des Ravatys (Saint Lager, France), originating from 18 countries of the world, with no information concerning the MLF achievement. Table Supplementary Information (S.I.) 1, 2 & 3 gathers information collected for the different analyzed wines.

2.2 Chemical analyses

Each wine was analyzed by the OenoFoss™ (Foss, Nanterre, France) analyser for classical oenological parameters: ethanol, total acidity, glucose, pH and volatile acidity. A Beckman® P/ACE 5000 capillary electrophoresis (Beckman Coulter, Brea, CA, USA) equipped with a UV detector was used to determine the amount of the four main organic acids in wine : tartaric acid, malic acid, lactic acid and citric acid following the methodology recommended by Organisation Internationale de la Vigne et du Vin (OIV, 2011). Polyphenolic compounds in wines were separated and quantified using an Acquity Waters UHPLC-DAD-fluorometer (Waters Corporation, Milford, MA, USA), using a previously described methodology (Coelho et al., 2019).

2.3 Wine Fluorescence measurements

All wines were diluted forty times with ultrapure water and poured in a 1 cm path-length quartz cuvette prior to steady state and time resolved spectroscopic measurements. For time-resolved fluorescence, five MLF+ wines and five MLF- wines were also diluted forty times with ultrapure water.

2.3.1 Steady state fluorescence

Excitation-Emission Matrices of Fluorescence (EEMF) were acquired on a Horiba Aqualog (Horiba Scientific, Kyoto, Japan) unit by setting the excitation wavelengths from 225 nm to 600 nm (3 nm interval) and the emission wavelengths from 200 to 600 nm (3.22 nm). Each EEMF was corrected daily for Rayleigh scattering and inner filtering and normalized to 1ppm quinine sulfate solution, using the constructor software (Aqualog software). All EEMF were gathered in a Chardonnay wine database and mathematically analyzed with a PARAFAC model using the Matlab (Mathworks, Natick, MA, USA) drEEM box (Murphy, Stedmon, Graeber, & Bro, 2013).

2.3.2 Time resolved fluorescence

Fluorescence decay measurements were performed using time-correlated single-photon counting (TCSPC) with a Horiba Jobin Yvon FluoroMax-4 (Horiba Scientific, Kyoto, Japan). Excitation was generated using a 950 ps pulsed 280 nm LED head source (DD-280L, pulse duration <1.5 ns) with a fixed working frequency of 1 MHz. We used a 280 nm diode instead of a 315 nm diode to be as close as possible to the maximum excitation with the pulsed light sources at our disposal. A Ludox® solution (Sigma Aldrich, Saint Louis, MI, USA) solution was used to daily calibrate the impulsional response function of the instrument. The fluorescence signal collected at emission maximum corresponding to PARAFAC component C4: 440 nm. In TCSPC the time difference between each photon detection and the corresponding excitation pulse is measured and stored into a histogram, showing the fluorescence decay after an excitation pulse. A total of 10000 photons were counted in the peak of each histogram before stopping the acquisition. Histograms were 4096 gates (4096 channels = 224.746 ns). The fluorescence decay was analyzed using the conventional exponential decay fitting function by the "DAS6 Analysis" analysis software (Horiba Scientific, Kyoto, Japan) and the phasor plot representation using the MAPI software (IRI, USR 3078 CNRS, BCF, available on request: http://biophotonique.univ-lille1.fr/spip.php?rubrique60) (Leray, Padilla-Parra, Roul, Héliot, & Tramier, 2013).

- **2.3.2.1. Exponential decay fitting**

If a uniform population of fluorophores are excited at a single excitation wavelength, the fluorescence intensity decay after an excitation pulse is described by a mono-exponential function, as follows:

$$F(t) = F_0 . e^{-t/\tau} \quad \text{(Equation 1)}$$

Where F(t) is the fluorescence intensity measured at time t, F_0 is the initial fluorescence intensity and τ is the fluorescence lifetime.

For complex samples, due to different fluorescent subpopulations and different chemical environments, a multi-exponential fitting procedure should be used to estimate as best as possible the number of fluorescent subpopulations contributing to the fluorescence decay curve. Such fitting procedures are validated by a "χ^2" (CHISQ) close to 1 (Moore, McCabe, & Craig, 2017).

In this study, we used a double exponential fitting function for all Chardonnay wines fluorescence decays, as follows:

$$F(t) = B_1 . e^{-t/\tau_1} + B_2 . e^{-t/\tau_2} \quad \text{(Equation 2)}$$

With $F_1 = B_1 / (B_1 + B_2)$ and $F_2 = B_2 / (B_1 + B_2)$

F(t) is the fluorescence intensity measured at time t, B_1 and B_2 are the pre-exponential factors, F_1 and F_2 the fractional intensities expressed in percentage, respectively for the subpopulations with fluorescence lifetimes τ_1 and τ_2 ($\tau_1 < \tau_2$).

- **2.3.2.2. Phasor plot representation**

The phasor plot is a graphical representation of all the raw TCSPC data in a vector space obtained by the mathematical Fourier transform decomposition. Each wine fluorescence decay curve is converted into [g ; s] coordinates, calculated by the cosine and sine transforms of the measured fluorescence intensity decay I(t), defined by:

$$g_{i,j}(\omega) = \frac{\int_0^T I(t) \cdot \cos(n\omega t) dt}{\int_0^T I(t)\, d(t)} \quad \text{(Equation 3)}$$

$$s_{i,j}(\omega) = \frac{\int_0^T I(t) \cdot \sin(n\omega t) dt}{\int_0^T I(t)\, d(t)} \quad \text{(Equation 4)}$$

Where ω is the laser repetition angular frequency, n is the harmonic frequency and T is the finite width of the temporal measurement window. For a mono-exponential decay, the [g ; s] coordinates are located on a semicircle centred on a point [0.5;0] with a radius 0.5. Whereas for a multi-exponential decay, the [g ; s] coordinates will no longer be located on the semicircle but rather inside this semicircle. In the semicircle, the short fluorescence lifetimes are close to the coordinates [1;0], and the long fluorescence lifetimes approach the origin [0;0].

Fluorescein (fluorescence lifetime: 4.1 ns) was used in the phasor plot representation for calibrating measurements between values obtained by exponential decay fitting and phasor plot analysis.

2.4. Statistical analysis

The measured oenological parameters, PARAFAC components Fmax values, fluorescence lifetimes and phasor plot g and s values of Chardonnay wines were statistically analyzed with a variance analysis (p-value <0.05) to evaluate the significance of differentiation between MLF+ and MLF- wines. This was conducted with Origin pro 8.0 software (OriginLab, Northampton, MA). Two types of multivariate analysis were carried out with SIMCA software (Umetrics, AB, Umea, Sweden): principal component analysis (PCA) with PARAFAC components Fmax with and without g and s values, and partial least square analysis (PLS) to evaluate the discrimination of MLF achievement in Chardonnay wines based on PARAFAC components Fmax values and g and s values obtained for the three typologies of Chardonnay wines (N=22).

3. Results and discussion

3.1 Wine chemical composition

Table 1 illustrates the chemical constituents that statistically differentiate wines according to MLF achievement among the 103 Chardonnay wines. Citric acid and pH were not significantly different. Tartaric acid, volatile acidity and glucose appeared to be significantly different between the two groups at 95% of confidence interval. Mean values of glucose concentrations were comprised between 2.59 and 3.03 $g.L^{-1}$, indicating that all wines are dry white wines. Total acidity, malic acid and lactic acid are the only three parameters that are significantly different at 99 % of interval of confidence. Mean values of ethanol and malic acid are higher in MLF- wines compared to MLF+ wines, respectively. Inversely, total acidity and lactic acid mean values are higher in MLF+ wines compared to MLF- wines. The great variability of provenance among the Chardonnay contest wines (Table S.I.3), led to a statistical differentiation of alcohol content in wines, principally due to grape maturity variability among all countries, but no differentiation in ethanol content is generally admitted. Results from fresh wines highlight the same tendency. Hence only the Total acidity and Malic/Lactic content of wines ~~are~~ truly statistically differentiate those wines. Additionally, for Chardonnay contest wines, the distinction between MLF+ and MLF- wines should be attenuated by the fact that malic and lactic acid could be added up to 4 $g.L^{-1}$ (expressed in tartaric acid equivalent) in musts and wines for acidification purposes according to OIV regulations (OIV, 2017). Some wines could have been bottled and stabilized while malolactic fermentation was still in progress.

Table 1 : Physicochemical parameters of wines for the 103 analyzed Chardonnay wines samples (A+B+C).

	MLF- wines	**MLF+ wines**
Alcohol (%v,v)	13.28 (0.83)	12.98 (0.67)*
pH	3.48 (0.14)	3.46 (0.14)
Glucose ($g.L^{-1}$)	2.59 (1.87)	3.03 (1.62)
TA ($g.L^{-1}$)	4.04 (0.42)	3.72 (0.34)**
Malic acid ($g.L^{-1}$)	2.56 (0.71)	0.52 (0.53)**
Lactic acid ($g.L^{-1}$)	0.39 (0.24)	3.59 (1.10)**
Tartaric acid ($g.L^{-1}$)	1.81 (0.57)	2.05 (0.54)*
Citric acid ($g.L^{-1}$)	0.50 (0.79)	0.61 (0.85)
N	50	53

*TA: total acidity expressed in tartaric acid equivalent per liter; N: number of wine samples; figures in parentheses, standard deviations; **: significant with p-value < 0.01 between the two groups of wines (MLF+/-); * : significant with p-value < 0.05 between the two groups of wines (MLF+/-).*

3.2 PARAFAC components describing Chardonnay wine diversity and sensitivity towards MLF achievement on full sample (A+B+C)

Fresh wines from two wineries (A and B), and Contest Chardonnay wines (C) were described by their EEMFs (examples of each group shown in Figure S.I.1). A wine PARAFAC model generates 4 PARAFAC components C1, C2, C3 and C4 describing all the analyzed wines (Figure 1). The PARAFAC model was pre-validated with a core consistency of 80% and further split half validated with four independent splits on the 4 component PARAFAC model, according to previously published procedures (Murphy et al., 2013). Figure 1A shows that the first two components of the PCA model cover 62.2 % of the fluorescence variability among the 103 analyzed wines. At a first glance, Chardonnay wines were heterogeneously distributed in terms of MLF achievement among these wines. Chardonnay wines from the two wineries A and B were clearly differentiated by means of their steady-state fluorescence. A less evident distinction appeared between fresh wines and wines from the Chardonnay wine contest. Such differentiation could be related to some particular attributes already discussed in literature (Coelho et al., 2015; Suciu, Zarbo, Guyon, & Magdas, 2019) gathering the vintage effect (2020 for the fresh wines compared to 2015-2017 for the contest wines) and the winemaking techniques (stabilization, fining, filtration, bottling and surely the bottle ageing enabling to differentiate Chardonnay fresh wines from bottled contest wines). Even if it was not the objective of the study, some wine origins were rather well discriminated among wines from the typology C, particularly when representing Fmax values of PARAFAC C3 against C4 (Figure S.I.2).

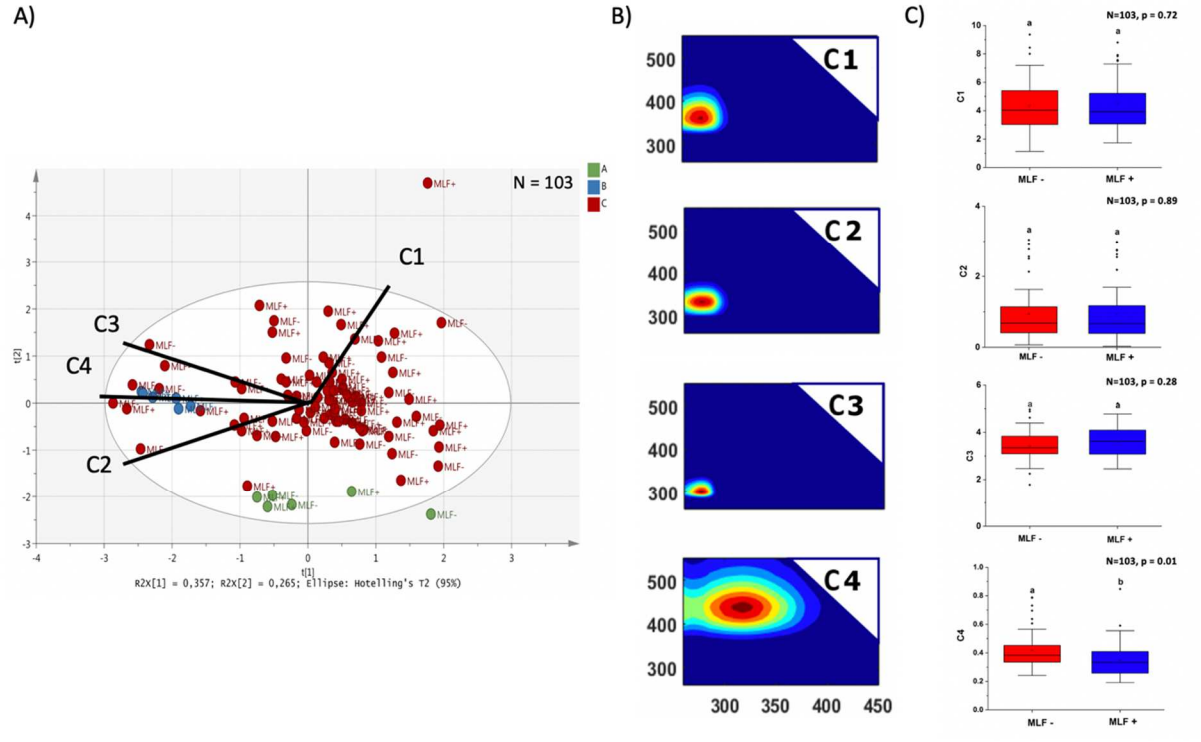

Figure 1 : Biplot representation of the first two components of a PCA model describing Fmax values of PARAFAC components for Chardonnay fresh wines from wineries A (green) and B (blue) and from Chardonnay wine contest C (red) (A). PARAFAC components EEMFs that were used as loadings for the PCA model (B). Analysis of variance of the four PARAFAC components Fmax values depending on the malolactic fermentation achievement (MLF+) or not (MLF-) (C). Different letters above box plot (a,b) represent significant differences (p=0.05) between the fermentative conditions.

EEMFs of the four PARAFAC components were generated with a PARAFAC model validated with a core-consistency diagnostic and a split-half validation made on four independent splits. They were in accordance with results from recent studies carried out on wines (Coelho et al., 2015; Elcoroaristizabal et al., 2016; Ranaweera et al., 2021; Suciu et al., 2019). We further study the ability of PARAFAC components to differentiate MLF achievement among wines, even though a global heterogeneity and variability from the wine provenance were previously discussed. Figure 1C shows the boxplot of the four PARAFAC components Fmax values. Within this variability and heterogeneity of Chardonnay wines: C1, C2 and C3 were not sensitive enough to distinguish the MLF achievement (same letter "a" between groups above the box plots). Nevertheless, PARAFAC component C4 Fmax values appeared to be statistically higher in MLF+ wines (0.41 +/- 0.14) compared to MLF- wines (0.34 +/- 0.12).

Previous studies highlighted this point among non-flavonoid compounds and more particularly tartaric esters of phenolic acids that are metabolized during MLF due to esterase activities present in several malolactic bacteria and liberating free phenolic and hydroxycinnamic acid derivatives (Cabrita et al., 2008; Collombel, Melkonian, Molenaar, Campos, & Hogg, 2019; Pérez-Martín, Seseña, Izquierdo, & Palop, 2013). As an example, caftaric acid has already been indicated as a good candidate with optical similarities and well correlated with PARAFAC component C4 but obviously this is not the only one ~~sole~~ (Roullier-Gall et al., 2017).

3.3 Fluorescence lifetime decay of PARAFAC component C4 in Chardonnay wines

3.3.1. Exponential decay fitting analysis of sample C

To interpret the discrimination between MLF- and MLF+ wines in terms of physico-chemistry of wine fluorophores behaving like the PARAFAC component C4 (Ex 315 nm/Em 440 nm) we investigate the fluorescence decays of wine fluorophores emitting at 440 nm when excited at 280 nm and not 315 nm for all this study. Figure 2 shows the fluorescence decays of MLF- and MLF+ Chardonnay wines, taken randomly from the Chardonnay contest wine series (C). They all present at least a bi-exponential decrease of intensity with short lifetimes $\boldsymbol{\tau}_1$ comprised between mean values of 4.19 ns and 4.53 ns and longer fluorescence lifetimes $\boldsymbol{\tau}_2$ comprised between 13.28 ns and 13.86 ns. Regardless of MLF achievement, fractional intensities were higher for the short fluorescence lifetime

297 τ_1 comprised between 61.1 and 63.7 % compared to 36.3 and 38.9 % for lifetime τ_2 showing this
298 general tendency for Chardonnay wines at constant pH equal to 5. This heterogeneous distribution of
299 fluorescence lifetimes indicated that fluorescence decay is not attributed to sole monomeric
300 fluorescent compound but also to condensed structures, which have already been associated with
301 flavonoids dimers (Bergmann, Barkley, Hemingway, & Mattice, 1987) and for polyphenolic
302 associations with proteins (Mueller-Harvey et al., 2012). Such chromophoric macromolecular
303 compounds derived from flavonoids or non-flavonoids should be present in Chardonnay white wines
304 (Coelho et al., 2017). The four mathematical parameters (τ_1, τ_2, F_1 and F_2) present no statistical
305 difference between MLF- and MLF+ wines, indicating that the fluorophores should reveal intimately
306 close environments related to an abundant phenolic population. Those wine emitting moieties are
307 characterized by a majority of short fluorescence lifetimes and they should be associated in larger
308 structures covalently bound or attached by interaction as reflected by the contribution of longer
309 fluorescence lifetimes.

A)

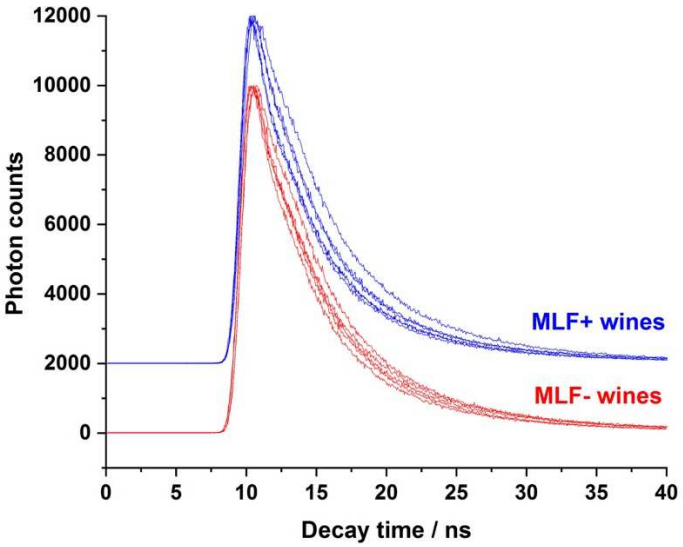

B)

	MLF- wines	MLF+ wines
τ_1 (ns)	4.19 (1.29)	4.53 (0.90)
τ_2 (ns)	13.28 (0.28)	13.86 (1.61)
F_1 (%)	61.1 (9.1)	63.7 (2.5)
F_2 (%)	38.9 (9.1)	36.3 (2.5)

310 *Figure 2 : Decay of fluorescence measured at pH=5 of MLF+ (blue) and MLF- wines (red) sampled during*
311 *Chardonnay wine contest C with an excitation wavelength set as 280 nm and emission set as 440 nm. The*
312 *baseline of the blue curve is shifted to better observe changes in fluorescence decay (A). Mean values of decay*
313 *lifetimes $\tau 1$ and $\tau 2$, expressed in ns and their associated fractional intensities F1 and F2 expressed in*
314 *percentage, as indicated in equation 2, at a fixed pH=5. Values in parenthesis indicate the mean standard*
315 *deviations for the five MLF+ wines (N=5) and MLF- wines (N=5) (B).*

316

317 **3.3.2. Phasor plot analysis**

318 For the following part, we use the (g,s) coordinates of wines to characterize fluorescence lifetime
319 decays of wines from wineries A (N=6) and B (N=6) and from Chardonnay wine contest C (N=10). This
320 type of analysis is commonly used in biology and medicine but has never been reported in food or

wine science to our knowledge. This approach better assesses heterogeneous fluorescence as encountered in wine environments (Ranjit, Malacrida, Jameson, & Gratton, 2018; Stringari, Cinquin, Cinquin, Digman, Donovan, & Gratton, 2011) and to depict physico-chemical interactions of fluorophores due to changes in pH, metal and metabolite concentration (Battisti, Digman, Gratton, Storti, Beltram, & Bizzarri, 2012; Celli, Sanchez, Behne, Hazlett, Gratton, & Mauro, 2010; Martelo, Fedorov, & Berberan-Santos, 2015). In our experimentation, the phasor plot approach helps to visualize the entire dataset of wine fluorescence decays dataset for MLF+/- wines. From the phasor plot (Figure 3) MLF+ wines appear to shift to higher g values. In order to validate this observation, we apply a variance analysis with a confidence interval of 95%. Mean values for the three typologies of wines are represented in the boxplot representations (Figure 3B, 3C, 3D and 3E). When all Chardonnay wines (N=22) are represented, g values are not statistically different between MLF- and MLF+ wines due to a high variability, even if a trend to higher g mean values is observed (from 0.60 to 0.62 in Figure 3B). This variability comes essentially from unfollowed fermentative processes during wine elaboration as observed in Figure 3E. Additional variability is brought by great discrepancies observed for g-values from winery A (Figure 3C) and winery B (Figure 3D) presenting mean g values of 0.65 and 0.55, respectively. Interestingly, for these fresh wines, regardless of the winery origin, MLF+ wines present systematically higher g mean values, meaning that wine fluorescence lifetimes decrease after the malolactic fermentation. This suggests the possibility of an input of wine quenchers during malolactic fermentation. This will be discussed in the next part in relation to wine acidic and polyphenolic composition (Table S.I.4).

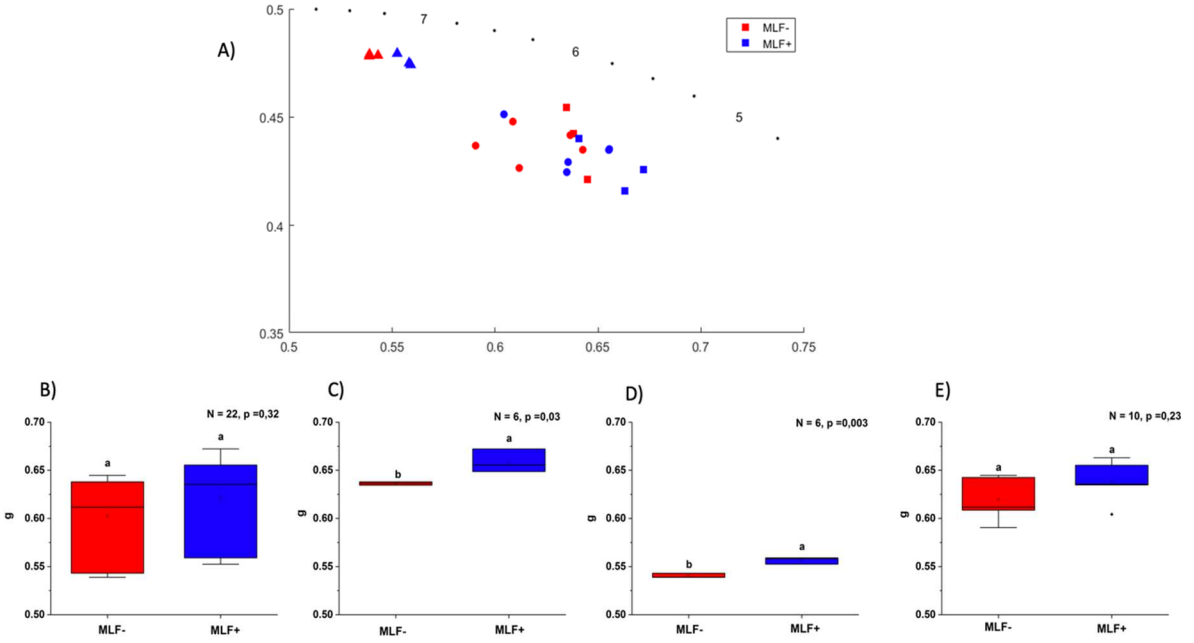

Figure 3: Phasor plot of fresh Chardonnay wines in winery A (squares), winery B (triangles) and Chardonnay contest wines C (circles) analyzed before and after malolactic fermentation, with an emission wavelength set at 440 nm for a fixed excitation at 280 nm (A). Chardonnay wines g values for all analyzed wines A+B+C (partly)

(N=22) (B), fresh wines from winery A (N=6) (C), fresh wines from winery B (N=6) (D) and a selection of Chardonnay contest wines (N=10) (E). Different letters above box plot (a,b) represent significant differences (p=0.05) between the fermentative conditions.

3.4. Discussion of potential quenchers occurring during malolactic fermentation in Chardonnay wines

In order to deepen wine fluorescence lifetime changes upon malolactic fermentation, g and s values were plotted for the 22 Chardonnay analyzed wines upon total acidity expressed in tartaric acid equivalent. A low correlation between g values and total acidity of each wine was found (correlation coefficient r= 0.36 and coefficient of determination R^2 = 0.1278, Figure S.I.3), strengthening the role of organic acid in the fluorescence lifetimes decreasing with an increase of organic acids in wines upon MLF. Nevertheless, the increase in total acidity upon malolactic fermentation is not suspected due to the metabolization of a stronger acid, malic acid into lactic acid. Generally, pH tends to increase with MLF but in our study the correlation was not good (correlation coefficient r= 0.06 and coefficient of determination R^2 = 0.0039, Figure S.I.4). Nevertheless, the study of wine pH on wine fluorophores should be carefully detailed in the future due to deprotonation of polyphenolic moieties, changing drastically the fluorophores lifetimes. We also look at the correlation with polyphenolic compounds without satisfactory results meaning that their concentration does not influence wine fluorescence lifetime measurement (results not shown here).

In order to understand the increase of g values during MLF, we supplement one MLF- fresh wine with potential acidic and polyphenolic quenchers at their determined concentrations in wines. Results are presented in Figure 4. It appears that all organic acids present a quenching effect towards fluorescence decay in a similar order of magnitude for concentrations ranging from 2 to 4 g/L. With increasing concentration of tartaric acid in wine from 4 to 5 and to 6 g/L, g values of MLF- wine increase at 0.700, 0.710, 0.715. This is in accordance with the positive correlation of g values of wines as a function of their total acidity (shown previously in Figure S.I.3). Interestingly caffeic acid and caftaric acid when supplemented at 10 mg/L in MLF- wine present a quite stronger quenching effect, as visualized by a g value reaching up to 0.737.

A)

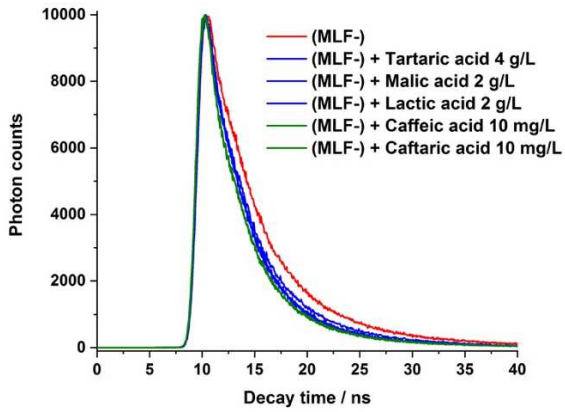

B)

Supplemented wines	g	s
(MLF-) wine	0.638	0.442
(MLF-) wine + Tartaric acid 4 g/L	0.700	0.416
(MLF-) wine + Malic acid 2 g/L	0.731	0.404
(MLF-) wine + Lactic acid 2 g/L	0.736	0.402
(MLF-) wine + Caffeic acid 10 mg/L	0.737	0.391
(MLF-) wine + Caftaric acid 10 mg/L	0.737	0.392

Figure 4: Fluorescence decays measured at pH=5 of a Chardonnay wine from winery A that has not achieved ~~realize~~ malolactic fermentation (MLF-) (red) and its supplemented wines with potential quenchers of wine fluorescence: organic acids (blue) and polyphenols (green) at realistic concentrations that could be encountered in Chardonnay wines (A). Table presenting g and s values from the phasor plot analysis of (MLF-) Chardonnay wine and supplemented wines fluorescence decays (B).

3.5. MLF distinction in Chardonnay wines (sample A+B+C) using multispectral fluorescence and chemometric analysis

Chardonnay wines multispectral fluorescence parameters generated by PARAFAC modeling and phasor plot analysis (PARAFAC components Fmax, g and s values) were interpreted with a multivariate analysis in order to discuss MLF achievement among wines depending on their typologies. Results are illustrated in Figure 5. The three categories of Chardonnay wines were clustered separately in Figure 5A, along PC1 (55.7%) and PC2 (20.8%), but with no visible separation in relation with MLF achievement. In order to gain significance in MLF distinction, a PLS-DA model was attempted on the same dataset (Figure 5B). The PLS model fits with a pretty good predictive ability Q^2Y = 0.632 (N=21, with an exclusion of one MLF- Chardonnay contest wine). Results show a clear discrimination of MLF- wines (blue) and MLF+ wines (red) regardless of the three typologies of wines. The loadings of the models are represented and confirmed the importance of values from PARAFAC component C4 Fmax values and g values for the optimization of the MLF separation among Chardonnay wines. Such combined multispectral data could be used in future for a better traceability among Chardonnay wines, particularly related to fermentative processes during winemaking. Further research could deepen multispectral fluorescence in wines to diagnose microbiological and chemical processes naturally occurring in wines that could impact its final quality. Such developments could be applied to other fermented food products and to research on adulteration and authentication issues.

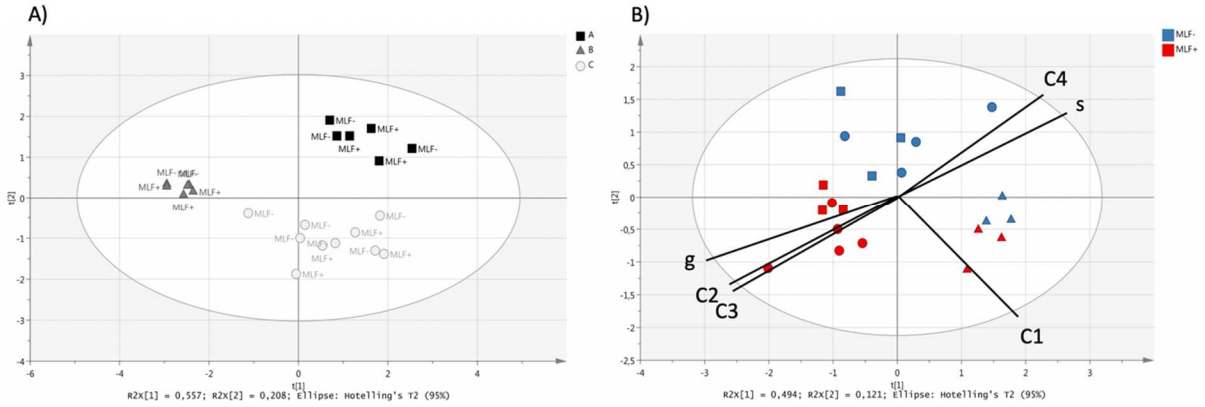

Figure 5: Biplot representation of the multispectral fluorescence Chardonnay wines from fresh wines from winery A (squares), winery B (triangles) and Chardonnay contest wines C (circles) obtained by a Principal component analysis (A) and by a Partial Least Square – Discriminant Analysis oriented on MLF achievement (B).

Conclusions

In conclusion, the combination of steady-state and time-resolved fluorescence techniques could be used to study the biochemical differences in Chardonnay wines. This study reveals that PARAFAC component C4 is a good biomarker index for MLF realization in wines. Chardonnay wine fluorophores with similar optical characteristics to the PARAFAC component C4 have been characterized at pH=5, by two fluorescence lifetimes: τ1 (4.19 - 4.53 ns) and τ2 (13.28 to 13.86 ns), respectively with two fractional intensities: F1 (61.1-63.7) and F2 (38.9-36.3). By applying a phasor plot analysis, wine fluorescence decays could be easily described by their (g,s) coordinates. g values appeared to systematically increase under malolactic fermentation on Chardonnay wines. Such an increase has been discussed by a quenching effect on wine fluorophores, occurring after acidic and polyphenolic modifications after MLF achievement in Chardonnay wines. When combining multispectral fluorescence to chemometric analysis, (MLF+) wines were clearly separated from (MLF-) wines, regardless of the origin of wines. Results from this study could motivate further wine research to combine multidimensional fluorescence measurements to gain in traceability towards fermentative processes occurring during winemaking.

Acknowledgement

The authors wish to acknowledge the research support of the FEDER Funding council and Horiba for their equipment support. We thank Y. Thierry, C. Bossuat and H.L. Arnould for the wine sampling at Boisset, Domaine de l'université de Bourgogne and during the "Chardonnay du Monde 2018" wine contest, respectively. We also thank F. Bagala for electrophoresis analysis assistance and J. Billon for

carefully proof-reading and editing the manuscript. The authors also acknowledge the “Conseil régional de Bourgogne-Franche-Comté” for its funding.

References

Agati, G., D’Onofrio, C., Ducci, E., Cuzzola, A., Remorini, D., Tuccio, L., . . . Mattii, G. (2013). Potential of a Multiparametric Optical Sensor for Determining in Situ the Maturity Components of Red and White Vitis vinifera Wine Grapes. *Journal of Agricultural and Food Chemistry, 61*(50), 12211-12218. https://doi.org/10.1021/jf405099n.

Agati, G., Meyer, S., Matteini, P., & Cerovic, Z. G. (2007). Assessment of Anthocyanins in Grape (Vitis vinifera L.) Berries Using a Noninvasive Chlorophyll Fluorescence Method. *Journal of Agricultural and Food Chemistry, 55*(4), 1053-1061. https://doi.org/10.1021/jf062956k.

Airado-Rodríguez, D., Durán-Merás, I., Galeano-Díaz, T., & Wold, J. P. (2011). Front-face fluorescence spectroscopy: A new tool for control in the wine industry. *Journal of Food Composition and Analysis, 24*(2), 257-264. https://doi.org/https://doi.org/10.1016/j.jfca.2010.10.005.

Airado-Rodríguez, D., Galeano-Díaz, T., Durán-Merás, I., & Wold, J. P. (2009). Usefulness of Fluorescence Excitation−Emission Matrices in Combination with PARAFAC, as Fingerprints of Red Wines. *Journal of Agricultural and Food Chemistry, 57*(5), 1711-1720. https://doi.org/10.1021/jf8033623.

Bartowsky, E. J. (2005). Oenococcus oeni and malolactic fermentation – moving into the molecular arena. *Australian Journal of Grape and Wine Research, 11*(2), 174-187. https://doi.org/10.1111/j.1755-0238.2005.tb00286.x.

Battisti, A., Digman, M. A., Gratton, E., Storti, B., Beltram, F., & Bizzarri, R. (2012). Intracellular pH measurements made simple by fluorescent protein probes and the phasor approach to fluorescence lifetime imaging. *Chemical communications (Cambridge, England), 48*(42), 5127-5129. https://doi.org/10.1039/c2cc30373f.

Bauer, R., & Dicks, L. M. T. (2017). Control of Malolactic Fermentation in Wine. A Review. *2017, 25*(2), 15. https://doi.org/10.21548/25-2-2141.

Bergmann, W. R., Barkley, M. D., Hemingway, R. W., & Mattice, W. L. (1987). Heterogeneous fluorescence decay of (4 .fwdarw. 6)- and (4 .fwdarw. 8)-linked dimers of (+)-catechin and (-)-epicatechin as a result of rotational isomerism. *Journal of the American Chemical Society, 109*(22), 6614-6619. https://doi.org/10.1021/ja00256a009.

Cabrera-Bañegil, M., Valdés-Sánchez, E., Moreno, D., Airado-Rodríguez, D., & Durán-Merás, I. (2019). Front-face fluorescence excitation-emission matrices in combination with three-way chemometrics for the discrimination and prediction of phenolic response to vineyard agronomic practices. *Food Chemistry, 270*, 162-172. https://doi.org/https://doi.org/10.1016/j.foodchem.2018.07.071.

Cabrita, M. J., Torres, M., Palma, V., Alves, E., Patão, R., & Costa Freitas, A. M. (2008). Impact of malolactic fermentation on low molecular weight phenolic compounds. *Talanta, 74*(5), 1281-1286. https://doi.org/https://doi.org/10.1016/j.talanta.2007.08.045.

Celli, A., Sanchez, S., Behne, M., Hazlett, T., Gratton, E., & Mauro, T. (2010). The epidermal Ca(2+) gradient: Measurement using the phasor representation of fluorescent lifetime imaging. *Biophysical Journal, 98*(5), 911-921. https://doi.org/10.1016/j.bpj.2009.10.055.

Coelho, C., Aron, A., Roullier-Gall, C., Gonsior, M., Schmitt-Kopplin, P., & Gougeon, R. D. (2015). Fluorescence Fingerprinting of Bottled White Wines Can Reveal Memories Related to Sulfur Dioxide Treatments of the Must. *Analytical Chemistry, 87*(16), 8132-8137. https://doi.org/10.1021/acs.analchem.5b00388.

Coelho, C., Gougeon, R. D., Perepelkine, L., Alexandre, H., Guzzo, J., & Weidmann, S. (2019). Chemical Transfers Occurring Through Oenococcus oeni Biofilm in Different Enological Conditions. *Frontiers in Nutrition, 6*(95). https://doi.org/10.3389/fnut.2019.00095.

Coelho, C., Parot, J., Gonsior, M., Nikolantonaki, M., Schmitt-Kopplin, P., Parlanti, E., & Gougeon, R. D. (2017). Asymmetrical flow field-flow fractionation of white wine chromophoric colloidal matter. *Anal. Bioanal. Chem., 409*(10), 2757-2766. https://doi.org/10.1007/s00216-017-0221-1.

Collombel, I., Melkonian, C., Molenaar, D., Campos, F. M., & Hogg, T. (2019). New Insights Into Cinnamoyl Esterase Activity of Oenococcus oeni. *Frontiers in Microbiology, 10*(2597). https://doi.org/10.3389/fmicb.2019.02597.

Elcoroaristizabal, S., Callejon, R. M., Amigo, J. M., Ocana-Gonzalez, J. A., Morales, M. L., & Ubeda, C. (2016). Fluorescence excitation-emission matrix spectroscopy as a tool for determining quality of sparkling wines. *Food Chem., 206*, 284-290. https://doi.org/10.1016/j.foodchem.2016.03.037.

González-Centeno, M. R., Chira, K., & Teissedre, P. L. (2019). Use of oak wood during malolactic fermentation and ageing: Impact on chardonnay wine character. *Food Chemistry, 278*, 460-468. https://doi.org/https://doi.org/10.1016/j.foodchem.2018.11.049.

Hernández, T., Estrella, I., Carlavilla, D., Martín-Álvarez, P. J., & Moreno-Arribas, M. V. (2006). Phenolic compounds in red wine subjected to industrial malolactic fermentation and ageing on lees. *Analytica Chimica Acta, 563*(1), 116-125. https://doi.org/https://doi.org/10.1016/j.aca.2005.10.061.

Hernández, T., Estrella, I., Pérez-Gordo, M., Alegría, E. G., Tenorio, C., & Moreno-Arribas, M. V. (2007). Contribution of Malolactic Fermentation by Oenococcus Oeni and Lactobacillus Plantarum to the Changes in the Nonanthocyanin Polyphenolic Composition of Red Wine. *Journal of Agricultural and Food Chemistry, 55*(13), 5260-5266. https://doi.org/10.1021/jf063638o.

Leray, A., Padilla-Parra, S., Roul, J., Héliot, L., & Tramier, M. (2013). 827Spatio-Temporal Quantification of FRET in Living Cells by Fast Time-Domain FLIM: A Comparative Study of Non-Fitting Methods. *PLOS ONE, 8*(7), e69335. https://doi.org/10.1371/journal.pone.0069335.

Longin, C., Petitgonnet, C., Guilloux-Benatier, M., Rousseaux, S., & Alexandre, H. (2017). Application of flow cytometry to wine microorganisms. *Food Microbiology, 62*, 221-231. https://doi.org/https://doi.org/10.1016/j.fm.2016.10.023.

Martelo, L., Fedorov, A., & Berberan-Santos, M. N. (2015). Fluorescence Phasor Plots Using Time Domain Data: Effect of the Instrument Response Function. *The Journal of Physical Chemistry B, 119*(32), 10267-10274. https://doi.org/10.1021/acs.jpcb.5b00261.

Martínez-Pinilla, O., Martínez-Lapuente, L., Guadalupe, Z., & Ayestarán, B. (2012). Sensory profiling and changes in colour and phenolic composition produced by malolactic fermentation in red minority varieties. *Food Research International, 46*(1), 286-293. https://doi.org/https://doi.org/10.1016/j.foodres.2011.12.030.

Mierczynska-Vasilev, A., Bindon, K., Gawel, R., Smith, P., Vasilev, K., Butt, H.-J., & Koynov, K. (2021). Fluorescence correlation spectroscopy to unravel the interactions between macromolecules in wine. *Food Chem., 352*, 129343. https://doi.org/10.1016/j.foodchem.2021.129343.

Moore, D. S., McCabe, G. P., & Craig, B. A. (2017). *Introduction to the Practice of Statistics.* (9th ed.).

Moret, F., Lemaître-Guillier, C., Grosjean, C., Clément, G., Coelho, C., Negrel, J., . . . Adrian, M. (2019). Clone-Dependent Expression of Esca Disease Revealed by Leaf Metabolite Analysis. *Frontiers in Plant Science, 9*(1960). https://doi.org/10.3389/fpls.2018.01960.

Mueller-Harvey, I., Feucht, W., Polster, J., Trnková, L., Burgos, P., Parker, A. W., & Botchway, S. W. (2012). Two-photon excitation with pico-second fluorescence lifetime imaging to detect nuclear association of flavanols. *Analytica Chimica Acta, 719*, 68-75. https://doi.org/https://doi.org/10.1016/j.aca.2011.12.068.

Murphy, K. R., Stedmon, C. A., Graeber, D., & Bro, R. (2013). Fluorescence spectroscopy and multi-way techniques. PARAFAC. *Analytical Methods, 5*(23), 6557-6566. https://doi.org/10.1039/C3AY41160E.

OIV. (2011). *Recueil des Méthodes Internationales d'Analyse des Boissons Spiritueuses d'Origine Vitivinicole. Méthode OIV-MA-AS313-19 : R2011, resolution OIV-Oeno 407-2011.*

OIV. (2017). *International Code of oenological practices. OIV Code Sheet - Issue 2017/01*.

Pérez-Martín, F., Seseña, S., Izquierdo, P. M., & Palop, M. L. (2013). Esterase activity of lactic acid bacteria isolated from malolactic fermentation of red wines. *International Journal of Food Microbiology, 163*(2), 153-158. https://doi.org/https://doi.org/10.1016/j.ijfoodmicro.2013.02.024.

Ranaweera, R. K. R., Gilmore, A. M., Capone, D. L., Bastian, S. E. P., & Jeffery, D. W. (2021). Spectrofluorometric analysis combined with machine learning for geographical and varietal authentication, and prediction of phenolic compound concentrations in red wine. *Food Chemistry, 361*, 130149. https://doi.org/https://doi.org/10.1016/j.foodchem.2021.130149.

Ranjit, S., Malacrida, L., Jameson, D. M., & Gratton, E. (2018). Fit-free analysis of fluorescence lifetime imaging data using the phasor approach. *Nature Protocols, 13*(9), 1979-2004. https://doi.org/10.1038/s41596-018-0026-5.

Robert-Peillard, F., Boudenne, J.-L., & Coulomb, B. (2014). Development of a simple fluorescence-based microplate method for the high-throughput analysis of proline in wine samples. *Food Chem., 150*, 274-279. https://doi.org/10.1016/j.foodchem.2013.10.135.

Roullier-Gall, C., Hemmler, D., Gonsior, M., Li, Y., Nikolantonaki, M., Aron, A., . . . Schmitt-Kopplin, P. (2017). Sulfites and the wine metabolome. *Food Chemistry, 237*, 106-113. https://doi.org/https://doi.org/10.1016/j.foodchem.2017.05.039.

Ruffner, H. P. (1982). Metabolism of tartaric and malic acids in Vitis: a review. Part B. *Vitis, 21*(4), 346-358.

Saad, R., Bouveresse, D. J.-R., Locquet, N., & Rutledge, D. N. (2016). Using pH variations to improve the discrimination of wines by 3D front face fluorescence spectroscopy associated to Independent Components Analysis. *Talanta, 153*, 278-284. https://doi.org/10.1016/j.talanta.2016.03.023.

Sadecka, J., Jakubikova, M., & Majek, P. (2018). Fluorescence spectroscopy for discrimination of botrytized wines. *Food Control, 88*, 75-84. https://doi.org/10.1016/j.foodcont.2017.12.033.

Santos, I. d., Bosman, G., Aleixandre-Tudo, J. L., & du Toit, W. (2022). Direct quantification of red wine phenolics using fluorescence spectroscopy with chemometrics. *Talanta, 236*, 122857. https://doi.org/10.1016/j.talanta.2021.122857.

Silva, G. T. M., da Silva, K. M., Silva, C. P., Rodrigues, A. C. B., Oake, J., Gehlen, M. H., . . . Quina, F. H. (2019). Highly fluorescent hybrid pigments from anthocyanin- and red wine pyranoanthocyanin-analogs adsorbed on sepiolite clay. *Photochemical & Photobiological Sciences, 18*(7), 1750-1760. https://doi.org/10.1039/C9PP00141G.

Stringari, C., Cinquin, A., Cinquin, O., Digman, M. A., Donovan, P. J., & Gratton, E. (2011). Phasor approach to fluorescence lifetime microscopy distinguishes different metabolic states of germ cells in a live tissue. *Proceedings of the National Academy of Sciences, 108*(33), 13582. https://doi.org/10.1073/pnas.1108161108.

Suciu, R.-C., Zarbo, L., Guyon, F., & Magdas, D. A. (2019). Application of fluorescence spectroscopy using classical right angle technique in white wines classification. *Scientific Reports, 9*(1), 18250. https://doi.org/10.1038/s41598-019-54697-8.

Trigueiro, P., Pedetti, S., Rigaud, B., Balme, S., Janot, J.-M., dos Santos, I. M. G., . . . Jaber, M. (2018). Going through the wine fining: Intimate dialogue between organics and clays. *Colloids and Surfaces B: Biointerfaces, 166*, 79-88. https://doi.org/https://doi.org/10.1016/j.colsurfb.2018.02.060.

Trivellin, N., Barbisan, D., Trivellin, N., Meneghesso, G., Meneghini, M., Zanoni, E., . . . Pastore, P. (2018). Study and Development of a Fluorescence Based Sensor System for Monitoring Oxygen in Wine Production: The WOW Project. *Sensors (Basel), 18*(4).

572 Wan, Y., Pan, F., & Shen, M. (2012). Identification of Jiangxi wines by three-dimensional fluorescence
573 fingerprints. *Spectrochim. Acta, Part A, 96*, 605-610.
574 https://doi.org/10.1016/j.saa.2012.07.030.
575 Zhong, X.-D., Fu, D.-S., Wu, P.-P., Liu, Q., Lin, G.-C., Cao, S.-H., & Li, Y.-Q. (2014). Rapid fluorescence
576 spectroscopic screening method for the sensitive detection of thiabendazole in red wine.
577 *Anal. Methods, 6*(18), 7260-7267. https://doi.org/10.1039/C4AY00991F.

578